

ORIGINAL ARTICLE

E2F1 loss induces spontaneous tumour development in Rb-deficient epidermis

C Costa, M Santos, M Martínez-Fernández, M Dueñas, C Lorz, R García-Escudero and JM Paramio

The specific ablation of *Rb1* gene in epidermis ($Rb^{F/F};K14cre$) promotes proliferation and altered differentiation but does not produce spontaneous tumour development. These phenotypic changes are associated with increased expression of E2F members and E2F-dependent transcriptional activity. Here, we have focused on the possible dependence on *E2F1* gene function. We have generated mice that lack *Rb1* in epidermis in an inducible manner ($Rb^{F/F};K14creER^{TM}$). These mice are indistinguishable from those lacking pRb in this tissue in a constitutive manner ($Rb^{F/F};K14cre$). In an E2F1-null background ($Rb^{F/F};K14creER^{TM}$; and $E2F1^{-/-}$ mice), the phenotype due to acute *Rb1* loss is not ameliorated by *E2F1* loss, but rather exacerbated, indicating that pRb functions in epidermis do not rely solely on *E2F1*. On the other hand, $Rb^{F/F};K14creER^{TM};E2F1^{-/-}$ mice develop spontaneous epidermal tumours of hair follicle origin with high incidence. These tumours, which retain a functional p19^{arf}/p53 axis, also show aberrant activation of β -catenin/Wnt pathway. Gene expression studies revealed that these tumours display relevant similarities with specific human tumours. These data demonstrate that the Rb/E2F1 axis exerts essential functions not only in maintaining epidermal homeostasis, but also in suppressing tumour development in epidermis, and that the disruption of this pathway may induce tumour progression through specific alteration of developmental programs.

Oncogene (2013) 32, 2937–2951; doi:10.1038/onc.2012.316; published online 13 August 2012

Keywords: skin; pRb; E2F1; p53; hair follicle; Wnt signalling

INTRODUCTION

The pRb tumour suppressor controls cell cycle progression, differentiation and apoptosis. Disruption of the 'Rb pathway' is a hallmark of most sporadic human cancers.¹ To avoid the embryonic lethality associated to generalized pRb loss and to study the *Rb1* roles *in vivo* in adult mice, multiple tissue-specific knock outs have been generated. The constitutive somatic elimination of *Rb1* gene in epidermis ($Rb^{F/F};K14cre$ mice) produces hyperproliferation and the disengagement of proliferation and differentiation processes, but is insufficient to allow tumour development.² Chemical carcinogenesis experiments in $Rb^{F/F};K14cre$ mice³ suggested a functional connection between pRb and p53 in epidermis, further demonstrated by the spontaneous skin tumorigenesis caused by the epidermal inactivation of p53 and pRb.⁴ On the other hand, p107 partially compensates *Rb1* loss avoiding some of the p53-mediated proapoptotic processes, and acts as a tumour suppressor in the absence of pRb.^{2,5,6} Such overlapping activities are partially mediated by adaptation, due to chronic *Rb1* loss, leading to increased p107 levels. Accordingly, the acute loss of pRb, showing no p107 induction, conduces to a more severe phenotype *in vitro*.^{2,7}

Multiple functions of pRb are dependent on its ability to interact with different E2F transcription factor family members. Of the eight known E2F family members, E2F1, which is preferentially bound by pRb, is of particular relevance as it may exert oncogenic^{8,9} and tumour suppressor functions.^{10,11} Importantly, loss of E2F1 reduces tumorigenesis of *Rb1* heterozygous mice indicating that an important part of the tumour suppressor activities of pRb depends on its ability to repress E2F1.^{12,13} In the context of epidermis, there are few data indicating a primordial role for E2F

members in the maintenance of tissue integrity and homeostasis. *In vitro* experiments indicated that E2F1 and E2F4 has opposite functions in triggering epidermal differentiation.¹⁴ In contrast, *in vivo* data revealed minor or no effect due to E2F1 loss, as $E2F1^{-/-}$ mice do not display any evident epidermal phenotype with the exception of altered wound healing processes.¹⁵ Recently, functional genomic analyses have revealed that the Rb/E2F pathway could have essential roles in maintaining epidermal stem-cell quiescence.¹⁶ Importantly, E2F functions in epidermal stem cells may rely not only on Rb family, but also on the interaction with CCAAT-enhancer-binding proteins (C/EBP) transcription factors.¹⁷ However, whether these activities are dependent on specific E2F members remains to be determined.

Regarding the role of E2F1 in epidermal carcinogenesis, there is still some controversy. The E2F1 overexpression in transgenic mouse epidermis leads to spontaneous tumour development, which is accelerated by p53 loss.^{18,19} On the other hand, such transgenic expression of E2F1 was found to inhibit ras-driven skin carcinogenesis upon different chemical carcinogenesis protocols.^{20–22} Remarkably, some of these tumour suppressive functions depends on a functional p53/p19^{arf} axis, similarly to the data obtained in $Rb^{F/F};K14cre$ mice upon chemical carcinogenesis,³ and are mediated by both apoptotic and non-apoptotic processes.

In order to analyse all these aspects, concerning the possible difference between chronic and acute *Rb1* loss in adult mice and the possible dependence on E2F1 of pRb *in vivo* functions, we have generated a new mouse model lacking pRb in epidermis in an inducible manner, and combined it with complete *E2F1* ablation. Our data indicate that pRb functions in epidermis are

partially independent on E2F1. Remarkably, E2F1 acts as a tumour suppressor in the absence of pRb, as the $Rb^{F/F};K14creER^{TM};E2F1^{-/-}$ mice display spontaneous tumours.

RESULTS

Epidermal consequences of acute *Rb1* loss alone and in the absence of *E2F1*

As the loss of *Rb1* in an acute or chronic manner leads to different consequences in cultured primary cells including keratinocytes,^{2,7} we have generated $Rb^{F/F};K14creER^{TM}$ mice to eliminate *Rb1* gene from the epidermis in an inducible manner by tamoxifen application. In the absence of tamoxifen, the epidermis of these mice is identical to that of mice without cre expression (Figure 1a) and showed no phenotype. Acute *Rb1* loss in epidermis (induced by topical tamoxifen administration Supplementary Figure 1a), which is as efficient as the constitutive *K14cre* expression (Supplementary Figure 1b) led to a moderate hyperplasia (Figure 1c) that persisted for entire lifespan (not shown); however, no spontaneous tumours occurred over 1 year and half after pRb loss (see below).

To examine the significance of pRb-dependent functions in epidermis through E2F1, we crossed $Rb^{F/F};K14creER^{TM}$ with $E2F1^{-/-}$ mice to obtain $Rb^{F/F};K14creER^{TM};E2F1^{-/-}$ mice. In the absence of tamoxifen, $Rb^{F/F};K14creER^{TM};E2F1^{-/-}$ mice behaved as $E2F1^{-/-}$ mice and did not display any obvious phenotype (Figure 1b), indicating that E2F1 is dispensable for the normal skin development and homeostasis. The $Rb^{F/F};K14creER^{TM};E2F1^{-/-}$ also display epidermal hyperplasia (Figure 1d) and altered epidermal differentiation process. In $E2F1^{-/-}$ epidermis, as in a wild type (wt) epidermis, the expression of basal keratin 5 (K5) was confined to a single cell layer while K6 was restricted to hair follicles (Figures 1e–h, respectively). In $Rb^{F/F};K14creER^{TM};E2F1^{+/+}$ we observed a clear expansion of K5-expressing cells (Figure 1i), which in some cases expressed the early differentiation marker K10 (inset in Figure 1i) and the ectopic expression of K6 in the interfollicular epidermis (Figure 1j). Overall, the epidermal differentiation phenotype of $Rb^{F/F};K14creER^{TM};E2F1^{-/-}$ mice (Figures 1k and l) is similar to that observed in $Rb^{F/F};K14cre$ mice,² although in some areas we observed increased cell layers expressing K5 (inset in Figure 1k), partial reduction of K10, and larger patches of interfollicular epidermis showing K6 expression (Figure 1l). Epidermal thickness measurements (Figure 2a) also indicated that the hyperplasia produced by *Rb1* loss is also enhanced in $Rb^{F/F};K14creER^{TM};E2F1^{-/-}$ mice. In agreement, epidermal cell proliferation monitored by bromodeoxyuridine (BrdU) incorporation showed that, although the absence of E2F1 has no effect (Figures 2b and e) and $Rb^{F/F};K14creER^{TM}$ mice exhibited increased proliferation (Figures 2c and e), the BrdU incorporation in the epidermis of $Rb^{F/F};K14creER^{TM};E2F1^{-/-}$ mice (Figures 2d and e) was higher than that observed upon pRb loss. Notably, such augmented proliferation in both Rb-deficient genotypes ($Rb^{F/F};K14creER^{TM}$ and $Rb^{F/F};K14creER^{TM};E2F1^{-/-}$) persisted at extended periods of time after the induction of recombination (Figure 2e).

A possible explanation for the observed phenotype in $Rb^{F/F};K14creER^{TM};E2F1^{-/-}$ mice could be that other E2F members could exert the functions of E2F1 in its absence. We observed that most E2F genes were expressed in wt epidermis (Figure 3a). Importantly, the expression and the activity of the E2F transcription factors were altered in the absence of pRb in epidermis.^{2,16} As compensatory mechanisms usually implicate the upregulation of the genes that balance the loss of another specific gene,^{2,5,7,23} we monitored the relative expression of different E2F species in mouse epidermis in comparison with $Rb^{F/F};K14creER^{TM}$. Our findings showed no major increase in any E2F member (Figure 3b). Indeed, in agreement with the role of E2F1 in regulating other E2F members, we observed a predominant

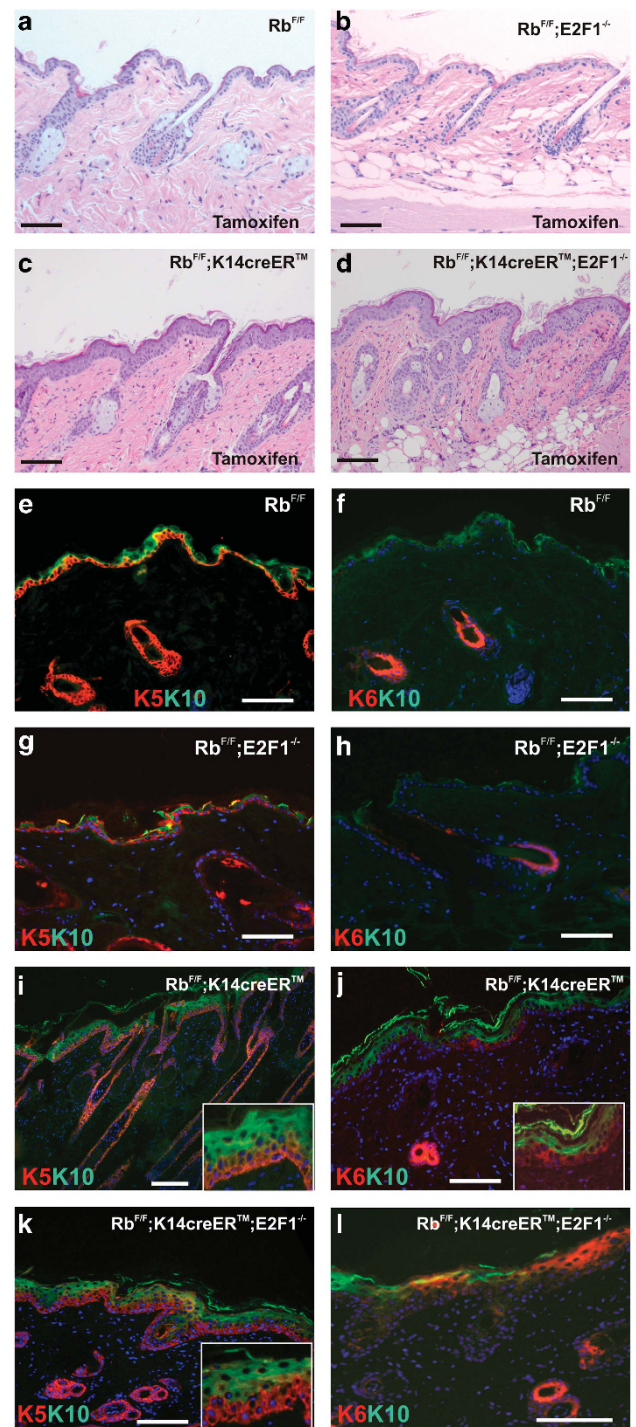


Figure 1. Epidermal phenotype of $Rb^{F/F};K14creER^{TM}$ and $Rb^{F/F};K14creER^{TM};E2F1^{-/-}$ mice. (a–d) H and E stained skin sections 2 months after tamoxifen treatment. (a) $Rb^{F/F}$, (b) $Rb^{F/F};E2F1^{-/-}$, (c) $Rb^{F/F};K14creER^{TM}$ and (d) $Rb^{F/F};K14creER^{TM};E2F1^{-/-}$. (e–l) Double immunofluorescence showing the expression of K5 (e, g, i, k), K6 (f, h, j, l) and K10 (e–l) in the epidermis of $Rb^{F/F}$ (e, f), $Rb^{F/F};E2F1^{-/-}$ (g, h), $Rb^{F/F};K14creER^{TM}$ (i, j) and $Rb^{F/F};K14creER^{TM};E2F1^{-/-}$ (k, l) mice 2 months after topical tamoxifen treatment. Antibodies are labelled in red or green colour according to the immunofluorescence they displayed in the corresponding sections. Insets show higher magnification images to illustrate the expansion of K5-positive basal layer and the expression of K6 in interfollicular epidermis in $Rb^{F/F};K14creER^{TM}$ and $Rb^{F/F};K14creER^{TM};E2F1^{-/-}$ mouse epidermis. Bars = 150 μ m.

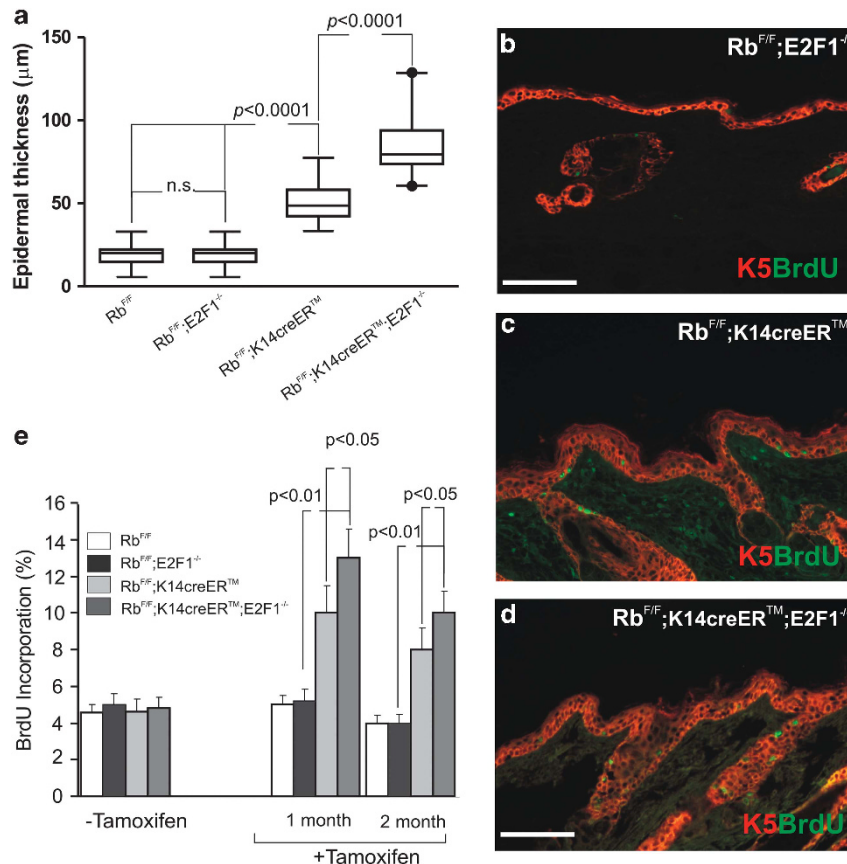


Figure 2. Epidermal proliferation in Rb^{F/F};K14creERTM and Rb^{F/F};K14creERTM;E2F1^{-/-} mice. (a) Epidermal thickness measure (in μm) mice of the quoted genotypes; Data come from the analysis of three different sections per mouse ($n = 5$) and are shown as mean \pm s.e. (b–d) Double immunofluorescence showing the expression of K5 and BrdU incorporation in the epidermis of Rb^{F/F};E2F1^{-/-} (b), Rb^{F/F};K14creERTM (c) and Rb^{F/F};K14creERTM;E2F1^{-/-} (d) mice. Antibodies are labelled in red or green colour according to the immunofluorescence they displayed in the corresponding sections. Bars = 150 μm (e) Quantitative analysis of BrdU incorporation in epidermis of the quoted genotypes. Data come from at least three mice per genotype scoring three different sections per mouse and are shown as mean \pm s.e.

reduction in several E2F species in Rb^{F/F};K14creERTM;E2F1^{-/-} epidermis. Of note, such reduction was absent in E2F1^{-/-} skin (Figure 3b). Western blot of primary keratinocytes corroborated these results, demonstrating no major increase in activator E2F members (Figure 3c), although a minor induction of repressor E2F3b and E2F4 were observed in double mutant cells (Figure 3c). In spite of these observations, luciferase experiments using an E2F-responding plasmid showed increased E2F-dependent activity by pRb loss, which is further augmented in Rb^{F/F};K14creERTM;E2F1^{-/-} keratinocytes (Figure 3d).

To gain information about possible molecular mechanisms that could explain the observed phenotypic differences, we performed a global gene expression analysis by microarrays. Comparison between normal and Rb^{F/F};K14creERTM;E2F1^{-/-} skin provided a gene expression signature of 3205-probe sets (1049 overexpressed and 2156 underexpressed in mutant skin; Supplementary Table 1). Unsupervised hierarchical clustering revealed the similarities between Rb^{F/F};K14creERTM and Rb^{F/F};K14creERTM;E2F1^{-/-} skin (Figure 4a), although some of the underexpressed or overexpressed genes in Rb^{F/F};K14creERTM skin display increased underexpression or overexpression in Rb^{F/F};K14creERTM;E2F1^{-/-} samples (denoted by brackets in Figure 4a). Consistent with the functional roles of the retinoblastoma family, most of the overexpressed genes in Rb^{F/F};K14creERTM and Rb^{F/F};K14creERTM;E2F1^{-/-} skin are involved in cell cycle regulation, DNA replication and repair (Figure 4b). However, other relevant functions, such as RNA splicing, translation and negative regulation of programmed cell death, were significantly represented. Chip enrichment

analysis²⁴ revealed that a very important fraction of the upregulated genes is bound by E2F transcription factors, as well as by other transcription factors with functional relevance in epidermis, embryonic stem-cell identity and in Wnt- and p53-dependent signalling (Figure 4c). On the other hand, the predominant functions of the underexpressed genes affect cell adhesion and migration, actin cytoskeleton and receptor tyrosine kinase, Wnt, and IGF signalling (Figure 4b).

Rb^{F/F};K14creERTM;E2F1^{-/-} mice develop spontaneous tumours

In spite of the increased proliferation and altered differentiation, the Rb^{F/F};K14creERTM mice did not display any sign of tumoral development over time. In contrast, in Rb^{F/F};K14creERTM;E2F1^{-/-} mice we observed the development of small lesions showing a wound-like appearance in the snout, legs, ears and back skin area (Figure 5a, and data not shown), whose histology (Figure 5b) identify as epidermal carcinomas. Tumours were first observed 2 months after tamoxifen treatment, and affected ~65% of the mice by 1 year after treatment (Figure 5c) with an incidence of 3.5 tumours per mouse, without increase with time (Figure 5d). As we did not detect any signs of tumour development in parental Rb^{F/F};K14creERTM or E2F1^{-/-} mice, or in Rb^{F/F};K14creERTM;E2F1^{-/-} mice in the absence of tamoxifen treatment (Figure 5c and data not shown), our findings indicated that the tumour suppressor activities of pRb are partially dependent on E2F1.

The histology the tumours (Figure 5b), showing dysplastic and hyperplastic hair follicles and hair-derived structures, suggested

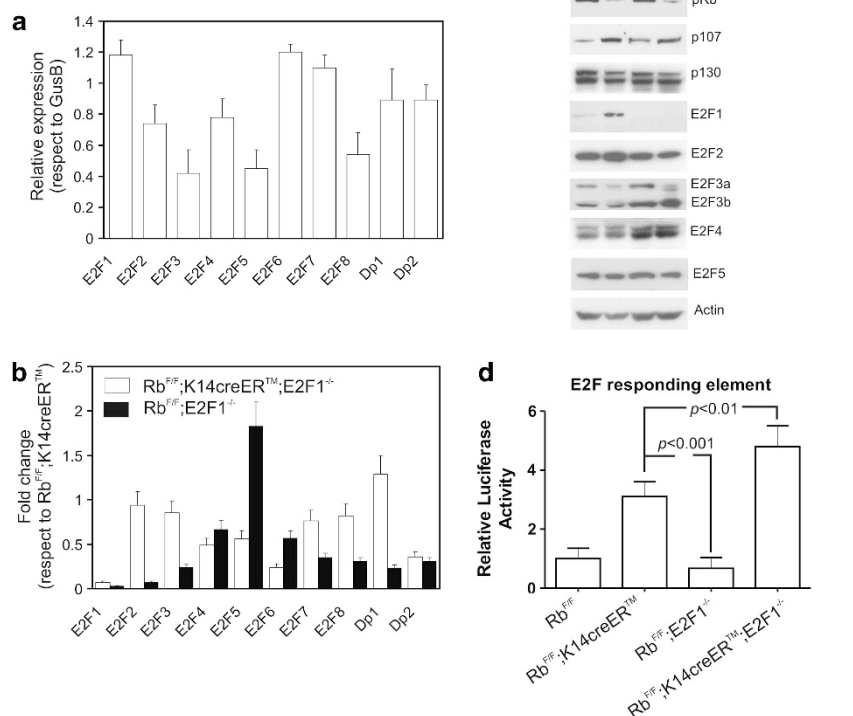


Figure 3. Comparative analysis of the expression of E2F family members. **(a)** Quantitative analysis of the relative expression of different E2F transcription factor family genes in wt skin using qPCR. *GusB* gene was used as a control for normalization. **(b)** Quantitative analysis of the relative expression of the different E2F transcription factor family genes in Rb^{F/F};K14creERTM;E2F1^{-/-} (open boxes) and Rb^{F/F};E2F1^{-/-} (black boxes) respect to Rb^{F/F};K14creERTM skin 2 months after topical tamoxifen treatment. **(c)** Western blot analysis of primary keratinocytes of the quoted genotype with or without 4OHTX treatment showing the expression of the indicated proteins. Actin was used as loading control. **(d)** Relative luciferase activity of E2F-responding elements in primary keratinocytes of the quoted genotypes (tamoxifen was added in all the cases). Data come from three independent experiments. The luciferase values were normalized to those obtained in control Rb^{F/F} keratinocytes and are shown as mean \pm s.e.m.

a possible hair follicle origin. In agreement, we observed the expression of hair follicle markers K6 (Figure 5e) K17 (Figure 5f), and K16 (not shown), in parallel with a reduction of interfollicular epidermal differentiation markers such K10 (Figures 5e and g) and generalized expression of K5 (Figure 5g) and p63 expression (Figure 5h). However, the hair matrix marker AE13 and trichohyalin (recognized by AE15 antibody²⁵), present in non-tumoral hair follicles of Rb^{F/F};K14creERTM;E2F1^{-/-} mice (not shown), were not detected in the tumours (Figures 5i and j), suggesting that these tumours had a possible hair follicle origin, but did not display a complete hair differentiation.

Possible molecular mechanisms underlying the development of Rb^{F/F};E2F1^{-/-} tumours

The tumours arising in Rb^{F/F};K14creERTM;E2F1^{-/-} mice were also characterized by increased proliferation, as demonstrated by BrdU incorporation (Figure 6a), and an almost insignificant apoptosis as analysed by terminal deoxynucleotidyl transferase dUTP nick end labeling (Figure 6b) and active caspase 3 (Supplementary Figures 2c and c'). The p19^{arf}/p53 axis, which is induced by the increased E2F1 expression and activity in Rb^{F/F};K14cre mice, is partially responsible for the reduced tumour sensitivity to chemical carcinogenesis of these mice^{3,26} and in transgenic

mice overexpressing E2F1 in epidermis.²² Increased expression of p19^{arf} (Figure 6c), primarily localized in the nucleoli (inset in Figure 6c), and a clear p53 induction were observed in most cells of Rb^{F/F};K14creERTM;E2F1^{-/-} tumours, opposite to the limited induction of p19^{arf} and p53 in scattered suprabasal cells in non-tumoral epidermis of Rb^{F/F};K14creERTM;E2F1^{-/-} mice (Supplementary Figures 2a and b). Western blot confirmed the induction of both p19^{arf} and p53 upon induction of pRb loss by tamoxifen treatment in Rb^{F/F};K14creERTM and Rb^{F/F};K14creERTM;E2F1^{-/-} primary keratinocytes (Figure 6e). Finally, luciferase experiments, using a p53-responding element, demonstrated the increase of p53 activity in Rb^{F/F};K14creERTM and Rb^{F/F};K14creERTM;E2F1^{-/-} keratinocytes after tamoxifen treatment (Figure 6f). Overall, these observations suggested that the spontaneous tumour development in Rb^{F/F};K14creERTM;E2F1^{-/-} mice is not attributable to impaired p19^{arf}/p53 axis activation.

The tumour suppressive functions of E2F1 in human colon cancer have been associated with its ability to inhibit the β -catenin-mediated transcriptional activities.²⁷ Moreover, in non-tumoral skin samples a relevant number of genes ($n = 173$, $P \leq 3 \times 10^{-22}$) bear β -catenin/TCF3 binding sites (Figure 4c). Accordingly, we hypothesized that spontaneous tumour of Rb^{F/F};K14creERTM;E2F1^{-/-} mice might be associated with alterations in β -catenin expression and/or localization. Moreover, the ectopic

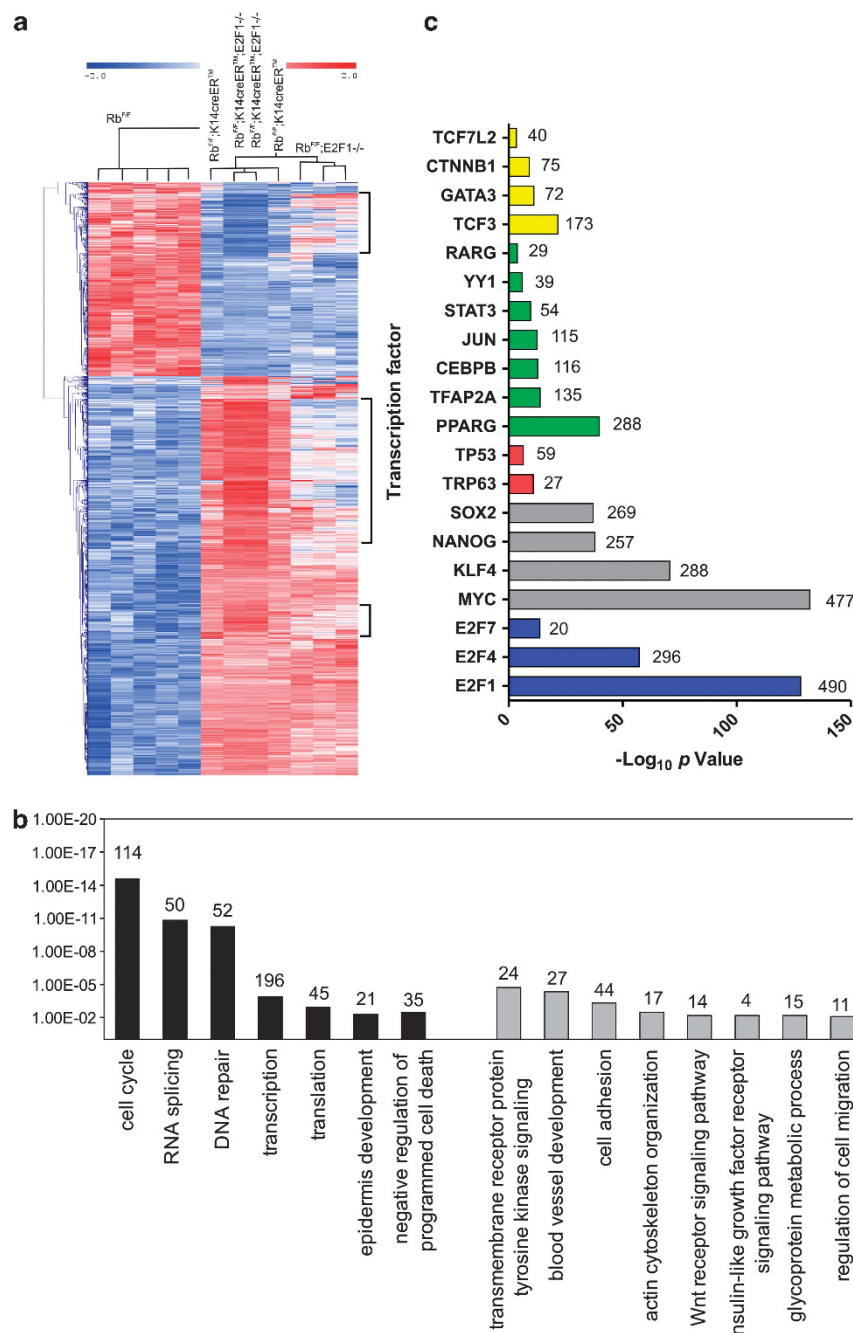
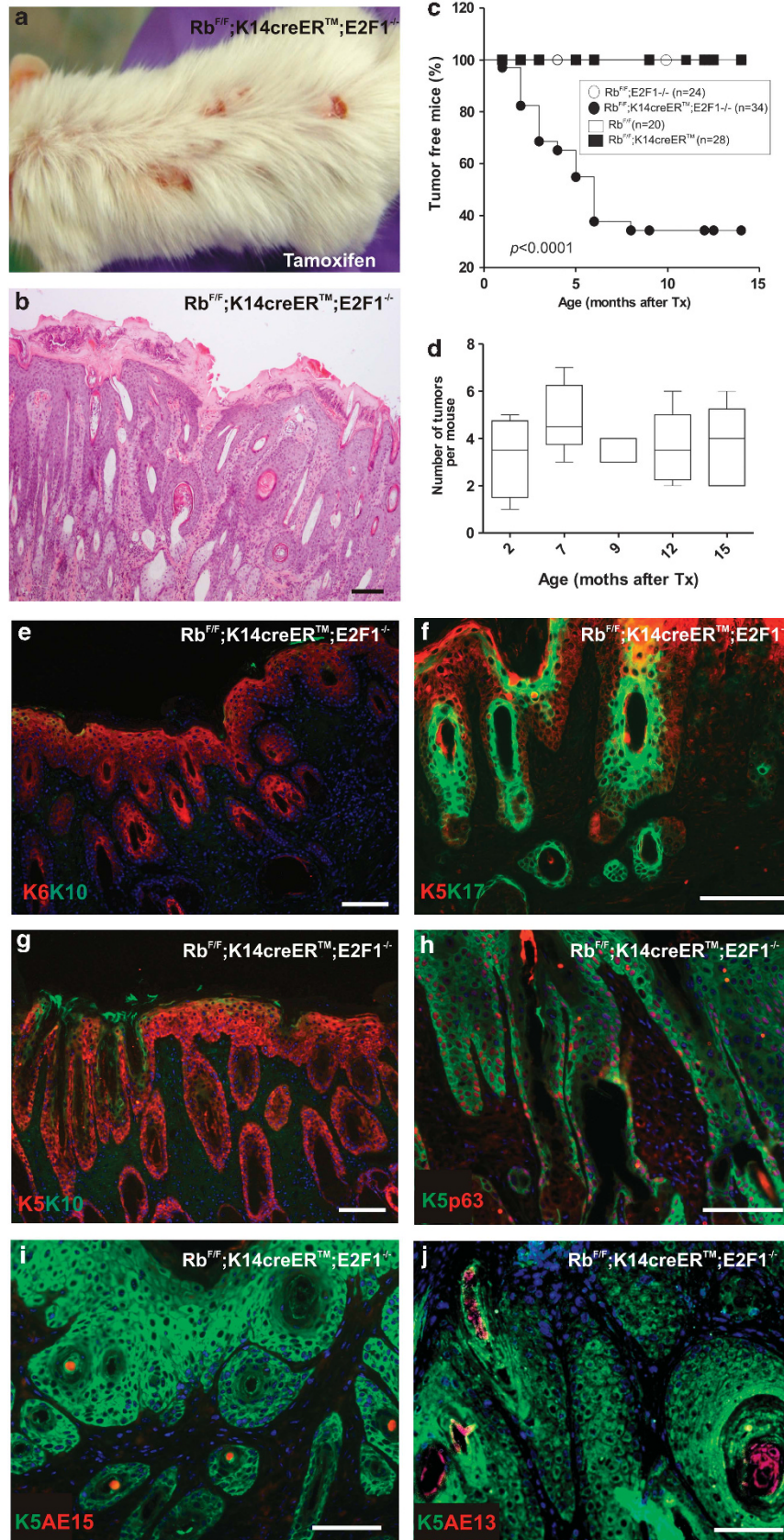


Figure 4. Genome-wide transcriptome analysis of Rb^{F/F};K14creERTM;E2F1^{-/-} mouse epidermis. **(a)** Unsupervised hierarchical clustering of mouse skin samples using the 3205-probe sets deregulated and differentially expressed between Rb^{F/F} and Rb^{F/F};K14creERTM;E2F1^{-/-} mouse epidermis. Note that Rb^{F/F};K14creERTM and Rb^{F/F};K14creERTM;E2F1^{-/-} samples clusterize together, although some genes underexpressed or overexpressed (denoted by brackets) display increased deregulation in Rb^{F/F};K14creERTM;E2F1^{-/-} mouse epidermal samples. **(b)** Enrichment analysis in Gene Ontology biological processes from the epidermal gene signature of Rb^{F/F};K14creERTM;E2F1^{-/-} mouse epidermis. The specific functions were plotted against the significance of enrichment assigned by the *P*-value. The numbers on top of each column represent the number of genes for each function. **(c)** Summary of Chip enrichment analysis analyses²⁴ showing the specific transcription factor binding to the overexpressed genes in Rb^{F/F};K14creERTM;E2F1^{-/-} mouse epidermis plotted against the corresponding significance of enrichment assigned by the *P*-value. The numbers on each column represent the number of genes for transcription factor.

expression of non-degradable β -catenin transgene in epidermis allows the development of hair follicle-derived tumours with impaired hair differentiation.^{28,29} We therefore studied the expression of total and active β -catenin in the epidermal tumours of Rb^{F/F};K14creERTM;E2F1^{-/-} mice. Immunohistochemistry analyses showed reduced β -catenin at the normal cell-cell contacts and increased nuclear localization of β -catenin in a

significant number of cells in Rb^{F/F};K14creERTM;E2F1^{-/-} tumours (Figures 7a and a'). Similar observations (Figures 7b and b') were obtained using an antibody that reacts with active β -catenin,³⁰ suggestive of transcriptional activation. In agreement, we observed the formation of outgrowths from hairs in pretumoral samples (Figure 7c), reminiscent of those formed by the expression of non-degradable β -catenin in transgenic mouse



epidermis.²⁸ We also found the increased nuclear and reduced cell-cell contact localization of β -catenin in these pretumoral samples (Figures 7d and d'). Further, luciferase experiments using

a β -catenin responding element revealed increased activity in Rb^{F/F};K14creERTM;E2F1^{-/-} keratinocytes after tamoxifen administration, which is further activated by the co-expression of Lef1

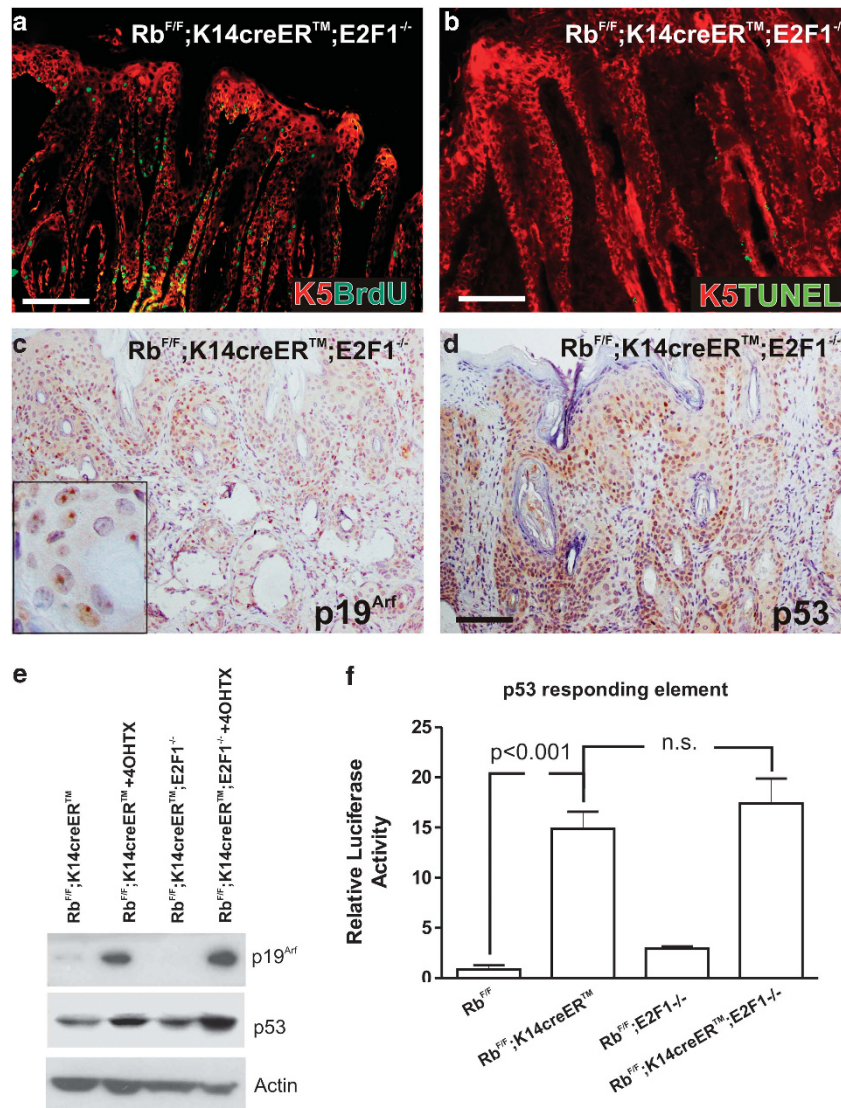


Figure 6. Proliferation, apoptosis and p19^{Arf}/p53 axis in Rb^{F/F};K14creERTM;E2F1^{-/-} tumours. (a) Representative immunofluorescence showing the expression of BrdU incorporation (green) and K5 expression (red) in Rb^{F/F};K14creERTM;E2F1^{-/-} tumours. Bar = 150 μ m (b) Representative immunofluorescence showing the terminal deoxynucleotidyl transferase dUTP nick end labeling positive staining (green) and K5 expression (red) in Rb^{F/F};K14creERTM;E2F1^{-/-} tumours. Bar = 150 μ m (c, d) Representative immunohistochemistry showing the induction of p19^{Arf} (c) (inset show higher magnification images to illustrate the nucleolar localization of p19^{Arf}) and p53 (d) in Rb^{F/F};K14creERTM;E2F1^{-/-} tumours. Bar = 150 μ m (e) Western blot analysis of primary keratinocytes of the indicated genotypes with or without 4OHTX treatment showing the expression of p19^{Arf} and p53 proteins. Actin was used as loading control. (f) Relative luciferase activity of p53-responding elements in primary keratinocytes of the quoted genotypes (tamoxifen was added in all the cases). Data come from three independent experiments. The luciferase values were normalized to those obtained in control Rb^{F/F} keratinocytes and are shown as mean \pm s.e.m.

Figure 5. Development of spontaneous tumours in Rb^{F/F};K14creERTM;E2F1^{-/-} mice. (a) Gross appearance of mouse back showing lesions in Rb^{F/F};K14creERTM;E2F1^{-/-} mice by 7 months after tamoxifen treatment. (b) H and E stained skin section of the lesions showing epidermal carcinomas of hair follicle morphology (Bar = 150 μ m). (c) Kaplan–Meier plot showing the incidence of tumours in Rb^{F/F}, Rb^{F/F};E2F1^{-/-}, Rb^{F/F};K14creERTM and Rb^{F/F};K14creERTM;E2F1^{-/-} mice. P-value was obtained by log-rank test. (d) Number of tumours per mouse throughout age represented as box plots showing median \pm s.d. (e–j) Representative immunofluorescences showing the expression of: hair marker K6 (red) and the early interfollicular differentiation marker K10 (green) (e); hair K17 (green) and basal keratinocyte K5 (red) (f); early interfollicular differentiation marker K10 (green) and basal keratinocyte K5 (red) (g); p63 (red) and basal keratinocyte K5 (green) (h); hair matrix marker AE15 (red) and basal keratinocyte K5 (green) (i); hair matrix marker AE13 (red) and basal keratinocyte K5 (green) (j) in Rb^{F/F};K14creERTM;E2F1^{-/-} tumours. (Bars = 150 μ m).

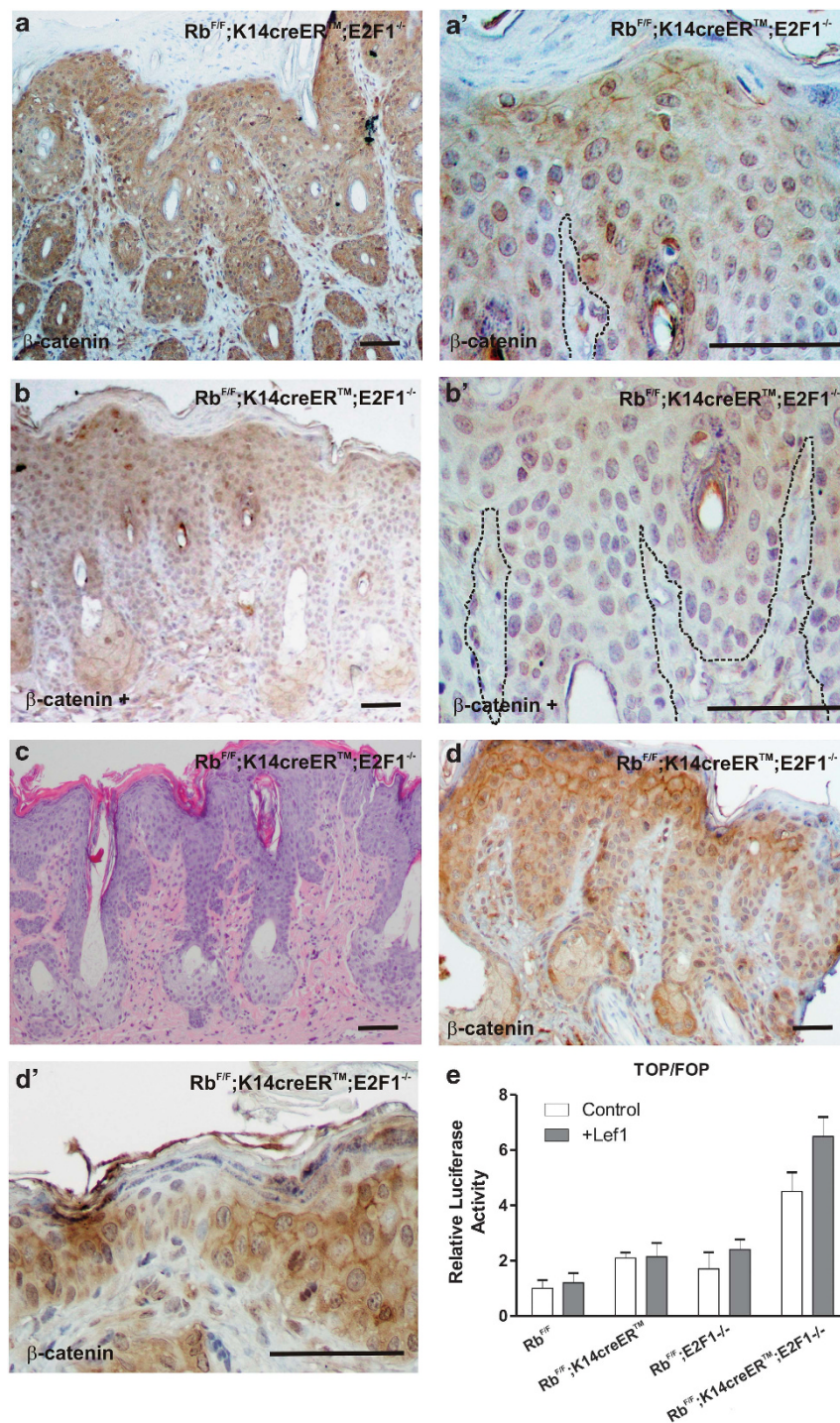


Figure 7. Rb^{F/F};K14creERTM;E2F1^{-/-} tumours display activated Wnt/ β catenin. (**a** and **a'**), Representative immunohistochemistry showing the expression of total β catenin in Rb^{F/F};K14creERTM;E2F1^{-/-} tumours. Bars = 150 μ m. (**b** and **b'**) Representative immunohistochemistry showing the expression of active β catenin in Rb^{F/F};K14creERTM;E2F1^{-/-} tumours. Bars = 150 μ m. (**c**) Example of H and E stained section showing precocious hair follicle formation and altered hair follicles in Rb^{F/F};K14creERTM;E2F1^{-/-} skin. Bar = 150 μ m. (**d** and **d'**) Representative immunohistochemistry of total β catenin expression in Rb^{F/F};K14creERTM;E2F1^{-/-} skin. Bars = 150 μ m (**e**) Relative luciferase activity of TOP/FOP reporter plasmid in primary keratinocytes of the quoted genotypes (tamoxifen was added in all the cases). Data come from three independent experiments. The luciferase values were normalized to those obtained in control Rb^{F/F} keratinocytes and are shown as mean \pm s.e.m. Where indicated, primary cells were also transfected with a Lef1 coding plasmid (see Materials and methods).

(Figure 7e). Next, the expression of several Wnt targets was monitored. Tumours displayed decreased expression of E-cadherin (Figure 8a) and increased expression of c-myc (Figure 8b), CyclinD1 (Figure 8c), Lgr5 (Figure 8d) and Sox9 (Figure 8e).

Quantitative reverse transcriptase-PCR (qRT-PCR) experiments (Figure 8g), confirmed the increased expression of *CcnD1*, *Sox9* and *Lgr5* genes and the reduced expression of *Cdh1* gene, and also showed the increased expression of multiple Wnt-target

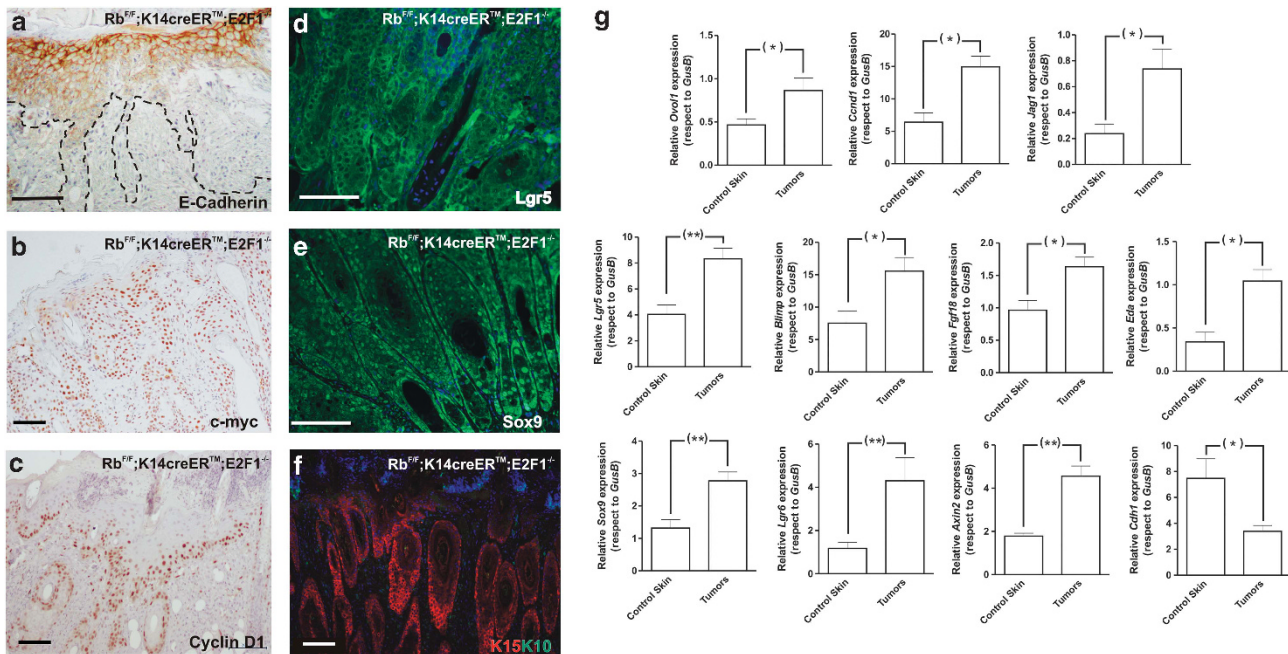


Figure 8. Wnt pathway is active in Rb^{F/F};K14creERTM;E2F1^{-/-} tumours. (a–c) Representative immunohistochemistry images showing the expression of E-cadherin (a), c-myc (b) and Cyclin D1 (c) in Rb^{F/F};K14creERTM;E2F1^{-/-} tumours. Dashed lines in (a) denote the boundaries of tumour mass. Bars = 150 μ m (d–f) Representative immunofluorescence showing the expression of the epidermal stem-cell markers Lgr5 (d), Sox9 (e) and K15 (f, in red) along with the interfollicular early differentiation marker K10 (green) in Rb^{F/F};K14creERTM;E2F1^{-/-} tumours. Bars = 150 μ m. (g) Quantitative analysis of the relative expression of different Wnt-dependent genes in control skin and tumours from Rb^{F/F};K14creERTM;E2F1^{-/-} mice using qPCR. *Gusb* gene was used as a control for normalization. Data come from the analysis of six control skin and eight different tumour samples and are shown as mean \pm s.e.m.

genes involved in hair follicle homeostasis, such as *Ovof1*, *Blimp*, *Fgf18*, *Eda*, *Lgr6* and *Axin2* (Figure 8g). Collectively these data confirm the involvement of active Wnt signalling in the spontaneous tumours in Rb^{F/F};K14creERTM;E2F1^{-/-} mice.

The Wnt/ β -catenin signalling is also an essential modulator of epidermal stem-cell activation.^{28,31,32} The increased expression of these genes in tumours may also indicate altered epidermal stem-cell homeostasis in Rb^{F/F};K14creERTM;E2F1^{-/-} mice. In agreement, we observed increased expression of K15 in the tumours (Figure 8f). The characterization of integrin α 6/CD34⁺ population by flow cytometry showed no significant differences among the genotypes, although a partial reduction was observed in E2F1^{-/-} mouse epidermis (Figure 9a). Similar observations were obtained when the expression and localization of K15- and CD34-positive cells was analysed by Immunofluorescence in telogen hair follicles of non-tumoral epidermis (Figure 9b–e). Nonetheless, although there is no major alteration in epidermal stem-cell compartment in Rb^{F/F};K14creERTM;E2F1^{-/-} compared with Rb^{F/F};K14creERTM mice, we observed the presence of aberrant dysplastic hair follicles with increased number of K15⁺/CD34⁺ cells (Figure 9f). In addition, increased number of mice showing anagen hairs was detected in Rb^{F/F};K14creERTM and Rb^{F/F};K14creERTM;E2F1^{-/-} mice older than 16 weeks, which presented asynchronous hair cycles. (Figure 9g). In support of these observations, the expression of Wnt-responding genes obtained from Transfac database, showed increased expression in non-tumoral skin samples from Rb-deficient samples (Rb^{F/F};K14creERTM and Rb^{F/F};K14creERTM;E2F1^{-/-}) (Supplementary Figure 3a). Similarly, when gene set enrichment analyses were performed between control and Rb^{F/F};K14creERTM;E2F1^{-/-} skin using a previously described epidermal stem-cell signature,¹⁶ we observed the reduced and increased expression of genes that are upregulated (61/654 transcripts; Supplementary Figure 3b) or downregulated (183/1630 transcripts; Supplementary Figure 3b'),

respectively, in epidermal CD34-positive stem cells. Together, these data may indicate that epidermal stem cells display altered homeostasis in Rb-deficient mice, but no clear differences were observed between Rb^{F/F};K14creERTM and Rb^{F/F};K14creERTM;E2F1^{-/-} mice.

Gene expression of Rb^{F/F};K14creERTM;E2F1^{-/-} tumours

Our above commented results indicate that the simultaneous absence of *Rb1* and *E2F1*, contrary to the absence of each gene alone, is able to promote the development of spontaneous tumours in stratified epithelia. To gain a better insight on the process and to analyse whether this may represent any type of human tumours, we performed gene expression analyses of these tumours and compared to normal skin. These studies rendered a gene list of 4925 probes (2865 overexpressed and 2060 underexpressed) (Figure 10a and Supplementary Table 2). Most of the tumour overexpressed genes are involved in cell cycle regulation, or DNA replication and repair, as well as mRNA and non coding RNA processing (Figure 10b), and also display a predominant involvement of E2F family and c-myc transcription factors (Figure 10c), while a moderate increase is observed for genes regulated by TCF3, GATA3 and β catenin (Figure 10c) as compared with non-tumoral skin analyses (Figure 4c). The underexpressed genes are primarily involved in metabolic processes, response to hormones, cytoskeleton organization and protein phosphorylation and localization (Figure 10b').

Next we analysed the functionality of p53-dependent pathway in the tumours. Gene Set Enrichment Analysis using a recently reported p53-dependent gene signature³³ revealed that, compared with non-tumoral skin, among the 1255 genes repressed by p53, 556 were induced in Rb^{F/F};K14creERTM;E2F1^{-/-} tumours (Supplementary Figure 4a). Conversely, among 1129 genes activated by p53, 400 were repressed in the

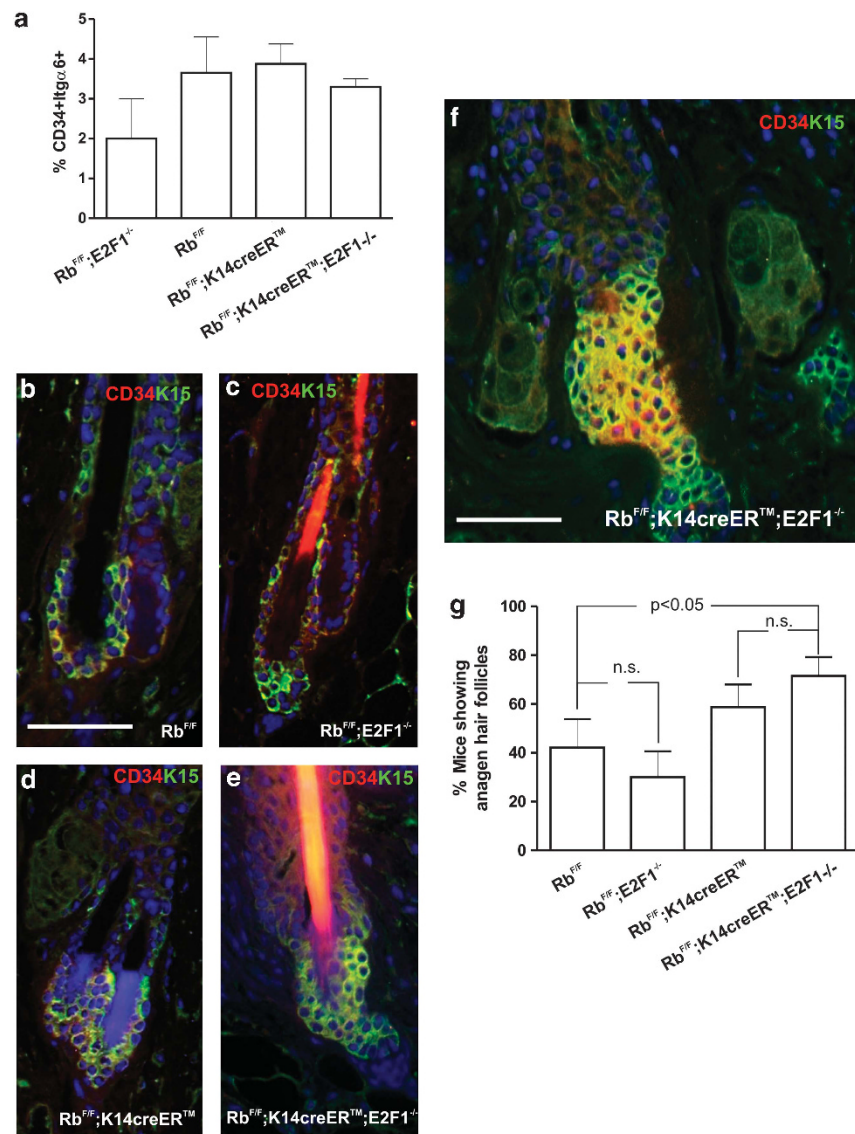


Figure 9. Epidermal stem cells in Rb^{F/F};K14creERTM;E2F1^{-/-} mice. **(a)** Percentage of integrin α6/CD34 + keratinocyte cell population in the quoted genotypes. Data come from the analysis of at least three independent isolation experiments and are shown as mean ± s.e.m. **(b–e)** Examples of double immunofluorescence images showing the expression of the cell stem markers K15 (green) and CD34 (red) in telogen hair follicles of Rb^{F/F} **(b)**; Rb^{F/F};E2F1^{-/-} **(c)**; Rb^{F/F};K14creERTM **(d)** and Rb^{F/F};K14creERTM;E2F1^{-/-} **(e)**. Bars = 150 μm. **(f)** Example of double immunofluorescence image showing the expression of the cell stem markers K15 (green) and CD34 (red) in a representative dysplastic hair follicle of Rb^{F/F};K14creERTM;E2F1^{-/-} mouse. Bar = 150 μm. **(g)** Summary of the analysis of the percentage of mice of the quoted genotypes showing anagen hair follicles. Data shown were obtained from the analysis of three different sections of back skin (1cm length each) per mouse (at least 25 animals were scored for each genotype) determining the presence of hair follicles in anagen. When at least 50% of hairs displayed anagen signs were considered positive.

Rb^{F/F};K14creERTM;E2F1^{-/-} tumours (Supplementary Figure 4b). These data suggest that, although p53 is induced in Rb^{F/F};K14creERTM;E2F1^{-/-} epidermal tumours (Figure 6), the p53-dependent response is partially impaired.

Finally, we studied any possible similarities between Rb^{F/F};K14creERTM;E2F1^{-/-} mouse tumours and human samples. To this we performed an exhaustive comparison of the over-expressed gene mouse tumour signature with gene data sets of human cancer samples using the Oncomine database.^{34,35} The highest significant overlap correspond to human bladder cancers (Figure 10d), and includes the comparison between normal and cancer samples, TP53 mutation and increased malignancy of the bladder cancer samples (Figure 10d). In agreement, we also observed significant decrease of E2F1 expression in bladder samples present in two different multicancer studies available in

Oncomine database (Supplementary Figure S5, Figure 10e and e'). Moreover, the reduced expression of E2F1 in bladder cancer samples was associated with Fibroblast growth factor receptor 3 mutation (Figure 10f) and tumour recurrence (Figures 10f' and f'').

Overall, these findings also support that the molecular events leading to the development of spontaneous tumours in Rb^{F/F};K14creERTM;E2F1^{-/-} mice, may also occur in specific human tumours.

DISCUSSION

In vitro experiments, including keratinocytes, have led to the hypothesis that acute loss of pRb could be more tumour prone than the chronic loss.^{2,7} In this case, adaptation allows the compensation among Rb family members, which can also explain

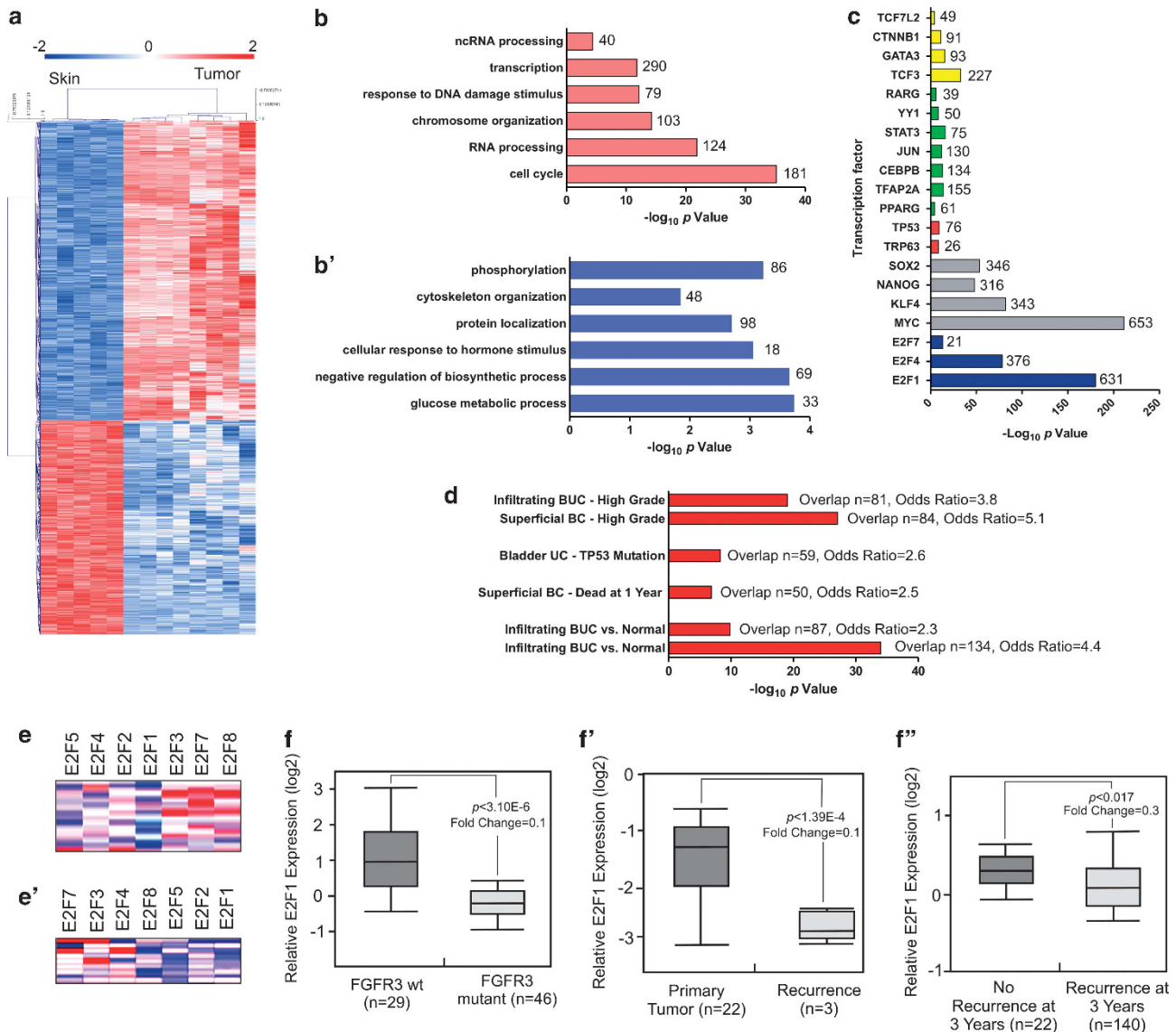


Figure 10. Genome-wide transcriptome analysis of Rb^{F/F};K14creERTM;E2F1^{-/-} mouse tumours. **(a)** Unsupervised hierarchical clustering of normal mouse skin and tumour samples using the 4925 transcript signature. probe sets deregulated and differentially expressed between Rb^{F/F} and Rb^{F/F};K14creERTM;E2F1^{-/-} mouse epidermis. **(b, b')** Enrichment analysis in Gene Ontology biological processes from the genes overexpressed **(b)** or underexpressed **(b')** in Rb^{F/F};K14creERTM;E2F1^{-/-} mouse tumours with respect to skin. **(b)** correspond to the overexpressed genes in tumours. The specific functions were plotted against the significance of enrichment assigned by the *P*-value. The numbers on top of each column represent the number of genes for each function. **(c)** Summary of Chip enrichment analysis analyses²⁴ showing the specific transcription factor binding to the overexpressed genes in Rb^{F/F};K14creERTM;E2F1^{-/-} mouse tumours plotted against the corresponding significance of enrichment assigned by the *P*-value. The numbers on each column represent the number of genes for transcription factor. **(d)** Summary of the overlapping between the 1000 more significant overexpressed genes in Rb^{F/F};K14creERTM;E2F1^{-/-} mouse tumours and the Oncomine database of human cancers.³⁴ See experimental procedures. **(e and e')** Heat map showing the expression of the quoted E2F family members in bladder tumours obtained from two different multicancer analyses (Bittner, E and Wooster, E; www.oncomine.org) available in Oncomine database (see Supplementary Figure S5). Blue colour indicate underexpressed and red overexpressed. Each horizontal bar represents a single sample. **(f and f')** Relative expression of E2F1 gene as showed by microarray studies on human bladder available in Oncomine database according to the presence of fibroblast growth factor receptor 3 mutation **(f)**, the comparison between primary tumour or recurrence **(f')**, and tumours showing or not recurrence after 3 years of follow-up.

the tumour suppressive functions of p107 in the absence of pRb.^{2,5} Our present data demonstrate that the acute loss of pRb induces phenotypic changes affecting proliferation and differentiation similar to those provoked by chronic loss,² but not tumour development. This indicates that the approach is not sufficient to analyse such acute effects *in vivo* and the induction of compensatory proteins occurred prior the possible tumour development.

The loss of pRb is associated in epidermis with increased expression and activity of different E2F proteins, including E2F1. This is further augmented by the loss of p107 protein, which also leads to spontaneous tumour development.^{2,5} We thus analysed whether the pRb functions in epidermis are dependent on E2F1. Our observations are in agreement with the lack of major alterations of epidermal differentiation and proliferation in the absence of E2F1 *in vivo*.¹⁵ Nonetheless,

a partial reduction of the CD34 + Itga6 + stem cell population was observed in E2F1^{-/-} mice, which might contribute to the delay of skin wound healing in these mice,¹⁵ and could also be related to the role of E2Fs in the maintenance of epidermal stem-cell identity mediated by C/EBP binding.¹⁷ On the other hand, the simultaneous absence of *Rb1* and *E2F1* not only does not ameliorate the pRb-deficient phenotype, but rather causes its partial enhancement, as demonstrated by the increased proliferation and the more evident signs of epidermal differentiation defects. This indicates that the epidermal phenotype due to *Rb1* loss does not result solely from the deregulation of the *E2F1* transcription factor. On the contrary, the clear phenotypic differences between E2F1^{-/-} and Rb^{F/F};K14creERTM;E2F1^{-/-} mouse epidermis would also suggest that the possible functions of E2F1 are almost completely dependent on pRb.

A possible explanation for the Rb^{F/F};K14creERTM;E2F1^{-/-} epidermal phenotype would include overlapping functions between E2F1 and other E2F members, similar to those observed between p107 and p130 pocket proteins in pRb absence.^{2,5,23} However, in spite of increased E2F-dependent activity, we did not detect increased expression of other E2F proteins in E2F1^{-/-} and Rb^{F/F};K14creERTM;E2F1^{-/-} mouse epidermis and keratinocytes. The future generation of other compound mutants in a pRb-deficient background may help to discern such possible compensative mechanisms.

The pRb tumour suppressor functions are partially mediated by its ability to bind different E2F transcription factor members, as demonstrated by the amelioration of the *Rb1* loss consequences by the subsequent ablation of different E2F members.³⁶⁻³⁸ Remarkably, the specific inactivation of E2F1 reduces tumorigenesis and extends the lifespan of mice bearing partial inactivation of *Rb1* gene,^{12,13} indicating that the Rb-E2F1 interaction is essential for this process. Our present data, showing spontaneous tumour development in Rb^{F/F};K14creERTM;E2F1^{-/-} mice, revealed that the Rb/E2F1 axis is essential for tumour suppression in epidermis, and suggested that, in this specific tissue setting, E2F1 might behave as a tumour suppressor in a context of pRb inactivation. Our gene expression data also extends this possibility, as a significant overlap between the upregulated genes in mouse tumours and human bladder tumours was observed. Moreover, multicancer database analysis revealed that in bladder cancer, where pRb is frequently inactivated,³⁹ E2F1 expression is frequently decreased, as previous immunohistochemistry studies suggested,⁴⁰ whereas a E2F-dependent gene signature identifies patients with high-risk superficial tumours that are likely to progress to invasive tumours.⁴¹ Future studies using clinical samples and mouse models bearing deletion of *Rb1* and *E2F1* genes in bladder would confirm this hypothesis.

The tumour suppressive functions of E2F1 in different tissues, including epidermis, have been associated with the induction of p19^{arf} and subsequent activation of p53.^{20,22,42} This process may also be responsible of the altered response of pRb-deficient epidermis challenged to chemical carcinogenesis protocols, in which E2F overactivation and p19^{arf} induction partially explain the increased p53 activation and expression.³ We observed p19^{arf} and p53 induction in Rb^{F/F};K14creERTM;E2F1^{-/-} tumours and cells, probably mediated by the activity of other E2F factors.^{43,44} Therefore, the loss of E2F1 promotes the development of epidermal tumours that retain the p19^{arf}/p53 tumour suppressor expression. Nonetheless, the transcriptome studies also indicated that the p53-dependent signalling pathway is partially impaired in the Rb^{F/F};K14creERTM;E2F1^{-/-} mouse tumours. This may also explain the reduced apoptosis observed. These findings warrant further studies on the molecular relationship between retinoblastoma family, p53 and E2F1 in the context of epithelial carcinogenesis.

The spontaneous tumours arising in Rb^{F/F};K14creERTM;E2F1^{-/-} mice display aberrant nuclear localization of β -catenin, and activation of the Wnt signalling. This is in agreement with the reported ability of E2F1 to inhibit β -catenin-dependent signalling in the gut.²⁷ However, pRb limits E2F1-mediated β -catenin repression activity in intestine, thus explaining the absence of mutations in *RB1* gene in colorectal tumours,²⁷ whereas the induction of nuclear β -catenin in epidermis occurs upon elimination of both *Rb1* and *E2F1* genes. Nonetheless, the functional connection between Rb family and Wnt-dependent signalling is probably broader than expected, as we have previously reported increased nuclear β -catenin in the absence of the retinoblastoma relatives p107 and p130.⁴⁵

The β -catenin/Wnt pathway has essential roles in the development and in tumorigenesis of multiple tissues⁴⁶⁻⁴⁸ including epidermis.^{28,31,49} Nuclear β -catenin localization, a hallmark of Wnt signalling, can drive hair follicle-derived tumours.^{28,29,49} The appearance of Rb^{F/F};K14creERTM;E2F1^{-/-} tumours as hair follicle-derived structures and the observation of some ectopic hair follicle like structures in Rb^{F/F};K14creERTM;E2F1^{-/-} epidermis also support the relevance of altered β -catenin localization in spontaneous tumour development. Also in agreement, we observed the increased expression of multiple Wnt-dependent genes in the Rb^{F/F};K14creERTM;E2F1^{-/-} tumours, including c-myc. Of note, tumour development in epidermis of transgenic mice expressing c-myc, is increased by *E2F1* loss,⁴² and a high number of genes overexpressed in the Rb^{F/F};K14creERTM;E2F1^{-/-} tumours display c-myc binding sites, thus indicating also a possible role of c-myc in tumour development.

The activation of Wnt signalling and increased c-myc expression disturbs epidermal stem-cell quiescence,^{29,50-53} whereas Rb/E2F axis promotes their quiescence.¹⁶ In agreement we found increased proportion of anagen follicles in adult animals, in spite of no major changes on the average number of epidermal stem cells. Nonetheless, the altered Wnt signalling pathway, the altered expression of genes associated with epidermal stem-cell identity and the presence of aberrant follicles showing increased K15 + CD34 + cell population also suggest the possible involvement of stem cells in tumour development in Rb^{F/F};K14creERTM;E2F1^{-/-} mice.

The possible role of Wnt signalling in tumour development may also explain the similarities between genes overexpressed in mouse tumours and human bladder cancers, in spite of their different tissue of origin. In this regard, β -catenin cooperates with several oncogenic insults to drive bladder cancer formation,⁵⁴⁻⁵⁶ and controls the homeostasis of bladder stem cells.^{57,58}

Collectively our present findings demonstrate a novel molecular mechanism that connects the loss of Rb and E2F1 to allow tumour development in mice. This process, which involves the Wnt signalling might be of relevance in certain human tumours. Consequently, our described Rb^{F/F};K14creERTM;E2F1^{-/-} mice could represent a perfectly suited tool to analyse the role of this pathway in tumorigenesis and in cancer stem cells in future research.

EXPERIMENTAL PROCEDURES

Mice

All animal experiments were approved by the Animal Ethical Committee and conducted in compliance with Centro de Investigaciones Energéticas, Medioambientales y Tecnológicas guidelines. The mouse model Rb^{F19/F19} has been previously described;² E2F1^{-/-} and K14creERTM were purchased from Jackson laboratory (Bar Harbor, ME, USA) (JaX 002785 and 005107, respectively). They were backcrossed for 10 generations to the inbred strain FVB/N genetic background. Tamoxifen treatment was topically administered in the shaved backskin of animals (2 × 2 cm) at 20 mg per day dissolved in dimethyl sulfoxide/acetone for 5 consecutive days. Primary keratinocytes were cultured as described.² One micromolar 4OHTX

diluted in ethanol was added to primary keratinocytes for 72 h in the culture medium.

Immunohistochemical methods

Immunohistochemistry or immunofluorescence analyses were performed as previously reported in formalin or ethanol-fixed paraffin embedded samples.^{4,59} High temperature antigen unmasking technique (10-min microwaving of slides in 0.01M citrate buffer) was used after deparaffinization to enhance the staining. Sections were then incubated with 5% horse serum for 30 min to block the Fc receptor in tissue, and then washed three times with sterile phosphate-buffered saline (pH 7.5) before incubation with the appropriate primary antibodies diluted in phosphate-buffered saline/bovine serum albumin. Antibodies used are anti K5, anti K6 (Covance, Princeton, NJ, USA), anti Sox9, anti Lgr5, anti p63, mouse monoclonal anti K10 (Santa Cruz Biotechnology, Santa Cruz, CA, USA), anti pRb (BD Pharmingen, Franklin Lakes, NJ, USA), anti β -catenin (Invitrogen, Carlsbad, CA, USA), anti active β -catenin (Millipore, Billerica, MA, USA), anti p19^{arf} (Abcam, Cambridge, UK), anti p53 (Novocastra, Newcastle, UK), anti CyclinD1, mouse monoclonal anti K15 (Neomarkers, Fremont, CA, USA), anti c-myc-P^{T58/S42} (Cell Signaling, Danvers, MA, USA), anti K17 (kindly provided by Dr P Coulombe) and AE13 and AE15 (kindly provided by Dr H Sung). Fluorochrome or Biotin-conjugated secondary antibodies were purchased from Jackson ImmunoResearch (West Grove, PA, USA). For immunohistochemistry, signal was amplified using avidin-peroxidase (ABC elite kit Vector, Vector labs, Burlingame, CA, USA) and peroxidase was visualized using diaminobenzidine as a substrate (DAB kit Vector, Vector labs). Control slides were obtained by replacing primary antibodies with phosphate-buffered saline (data not shown). Mice were injected intraperitoneally with BrdUrd (0.1 mg/g weight in 0.9% NaCl; Roche, Basel, Switzerland) 1 h before killing. BrdUrd incorporation was monitored by double immunofluorescence in ethanol-fixed or in formalin-fixed sections using an anti-BrdU antibody (Roche) as described.⁶⁰ Apoptosis was monitored using *In situ* Cell Death Detection Kit (Roche) according to the manufacturer's recommendations.

Western blot

Western blot was performed as described previously.^{2,4,59} Briefly, pelleted keratinocytes were disrupted by freeze-thawing cycles in lysis buffer (200 mM 4-(2-hydroxyethyl)-1-piperazineethanesulfonic acid pH 7.9, 25% glycerol, 400 mM NaCl, 1 mM ethylenediaminetetraacetic acid, 1 mM ethylene glycol tetraacetic acid, 1 μ g/ml aprotinin, 1 μ g/ml leupeptin, 1 mM phenylmethanesulfonyl fluoride, 20 mM NaF, 1 mM NaPPi, 1 mM Na₃VO₄, 2.5 mM dithiothreitol, and centrifuged to obtain supernatant containing total protein. Thirty five microgram protein per sample were resolved in sodium dodecyl sulfate—polyacrylamide gel electrophoresis, gels and transferred to nitrocellulose membranes (Amersham, Little Chalfont, UK). Membranes were blocked with 5% non-fat milk diluted in Tris-buffered saline (TBS) and incubated with the appropriate antibodies diluted in TBS-T 0.5% bovine serum albumin. Secondary antibodies were purchased from Jackson ImmunoResearch. Super Signal West Pico Chemiluminescence Substrate (Pierce) was used according to the manufacturer's recommendations to visualize the bands. Antibodies used are mouse monoclonal anti pRb (BD Pharmingen), anti p107, anti p130, anti E2F1, anti E2F2, anti E2F3, anti E2F4 and anti E2F5 (Santa Cruz Biotechnology), anti p19^{arf} (Abcam) and anti p53 (Novocastra). loading was controlled by using an anti Actin antibody (Santa Cruz Biotechnology).

Quantitative PCR

For the qPCR analyses, total RNA was isolated from mouse skin or tumour samples using RNeasy Mini Kit (Qiagen, Hilden, Germany) according to the manufacturer's instructions. Genomic DNA was eliminated from the samples by a DNase treatment (Rnase-Free Dnase Set, Qiagen). RNA from each sample (800 ng) was reverse transcribed in a final volume of 40 μ l using the Omniscript RT Kit (Qiagen) and an oligo (dT)₁₈ primer. Real time PCR was performed in a 7500 Fast Real Time PCR System (Applied Biosystems, Carlsbad, CA, USA) with 10 μ l reactions containing 5 μ l of Power SYBR GREEN PCR master mix (Applied Biosystems), 3 μ l or RNase-free water, 0.5 μ l of each primer (500 nM), and 1 μ l of complementary DNA as PCR template. Cycling parameters were 50 °C for 2 min, 95 °C for 10 min to activate DNA polymerase followed by 40 cycles of 95 °C for 15 s, and 60 °C for 1 min. The sequences of the specific oligonucleotides used are provided in Supplementary Table 3. Detection of fluorescence was carried out at the end of each amplification step. Moreover, melting curves were

performed to verify specificity of the target and the absence of primer dimerization after each amplification. Reaction efficiency was calculated for each primer combination and *GUS B* gene was used as reference gene.

Luciferase Assays

Luciferase experiments were performed essentially as described.² Primary keratinocytes were incubated for 48 h with 4-hydroxytamoxifen to induce pRb deletion. Transient transfections were performed with the superfect reagent (Qiagen) according to the manufacturer's protocol after 4-hydroxytamoxifen treatment. Thirty-six hours after transfection, cells were harvested for luciferase assays (Promega Dual-Luciferase Kit, Promega, Madison, WI USA). Firefly luciferase values were standardized to Renilla luciferase values (pRL-SV40; Promega) to account for differences in transfection efficiency between samples. As a control, the β catenin/Lef1 reporter (TOPflash), was replaced by a mutant (FOPflash) reporter to ensure that values were dependent on the Lef1/Tcf binding sites in the promoter (kindly provided by Dr JS Gutkind). Expression plasmid coding for Lef1 (kindly provided by Dr A Cano), pGL3-p53-responding elements (kindly provided by Dr I Palmero) and pGL3-E2F-responding elements (kindly provided by Dr X Lu) were used.

Flow cytometry

Keratinocyte populations from adult backskin were isolated 2 months after topical tamoxifen treatment from Rb^{F/F}, Rb^{F/F};K14cre^{ERTM}, Rb^{F/F};E2F1^{-/-} and Rb^{F/F};K14cre^{ERTM};E2F1^{-/-} mice to analyse CD34 and Itga6 surface expression as described.^{16,61,62} Cell suspensions were labelled with anti-CD34 (eBioscience, San Diego, CA, USA), washed in FACS Buffer (phosphate-buffered saline containing 5% foetal bovine serum), stained with anti-rat PE (Jackson ImmunoResearch), anti-Itga6 antibody directly conjugated to FITC (BD Pharmingen). Cells were analysed in an EPICS XL flow cytometer (Coulter Electronics, Hialeah, FL, USA).

Genome-wide transcriptome analyses.

RNA was obtained from skin samples and tumours, and purified from as previously described.^{4,5,23} Hybridization was done to Affymetrix Mouse GE MOE430 2.0 array (Affymetrix, Santa Clara, CA, USA). Raw and processed data were deposited in the GEO database (GSE38048). Supervised analysis of differential expression between tumours and normal tissue was done using t-test using Bonferroni correction and all available random permutations using the open source software multiexperiment viewer.⁶³ Unsupervised hierarchical clustering using the different gene signatures was done with Pearson distance metrics and complete linkage method. Z-scores in log2 scale were calculated for heatmap visualization. MOE430 2.0 Affymetrix chip probe set IDs were mapped to human using Ailun web utility.⁶⁴ Enrichment analysis of Gene Ontology terms was done upon uploading selected probe sets identifiers into DAVID Functional Annotation web tool, which computes enrichment of Gene Ontology biological processes terms using EASE score.^{65,66} ChIP enrichment analyses²⁴ were performed using the Chip enrichment analysis web tool without filtering and transcription factors providing a *P*-value ≤ 0.001 were manually curated.

Enrichment analysis of p53-regulated genes

Gene Set Enrichment Analysis⁶⁷ was used to analyse the enrichment of epidermal stem-cell gene signature¹⁶ comparing normal control and Rb^{F/F};K14cre^{ERTM};E2F1^{-/-} mouse epidermis. Similar approach was used to determine the expression of p53-activated and p53-repressed DNA damage response genes within the mouse tumours when compared with normal skin. Gene sets, as determined by both ChIP-seq and transcriptome microarray data were downloaded from Li *et al.*³³ We permuted the gene set for 1000 times rather than permutating the phenotype because the sample number is small.

Overlapping analysis in human cancer gene expression studies

We used Oncomine gene expression signatures database to search for overlapping.³⁴ Association of the mapped signatures with the database signatures was tested using Fisher's exact test, and was considered significant for odds ratio > 2 , and *P*-value < 0.001 . Genes overexpressed in the mouse carcinomas were mapped to human gene symbols and loaded into the oncomine database. We have searched for overlaps using different filtering criteria, based on the type of human cancer comparison performed. These criteria were: (i) 'cancer vs normal', to search for

similarities with human tumours of different tissue of origin; (ii) 'Mutation', to search for similarities with human cancer samples characterized by specific gene mutations; and (iii) 'clinical outcome', to search for similarities with human cancer with different clinical characteristics. The expression of E2F transcription factor family genes was performed in OncoPrint using 'Multicancer' criteria.

CONFLICT OF INTEREST

The authors declare no conflict of interest.

ACKNOWLEDGEMENTS

Ministerio de Ciencia e Innovación (MICINN) grants SAF2006-0121, SAF2011-26122-C02-01 and JCI-2010-06167, Comunidad Autónoma de Madrid Oncology Program Grant S2006/BIO-0232 and: CAM P2010/BMD-2470, Ministerio de Sanidad y Consumo grant ISCIII-RETIC RD06/0020/0029 and from Fundación Sandra Ibarra to JMP. The excellent technical support by Pilar Hernández in histology and the personnel of the CIEMAT Animal Facility are specially acknowledged.

REFERENCES

- Nevins JR. The Rb/E2F pathway and cancer. *Hum Mol Genet* 2001; **10**: 699–703.
- Ruiz S, Santos M, Segrelles C, Leis H, Jorcano JL, Berns A et al. Unique and overlapping functions of pRb and p107 in the control of proliferation and differentiation in epidermis. *Development* 2004; **131**: 2737–2748.
- Ruiz S, Santos M, Lara MF, Segrelles C, Ballestin C, Paramio JM. Unexpected roles for pRb in mouse skin carcinogenesis. *Cancer Res* 2005; **65**: 9678–9686.
- Martinez-Cruz AB, Santos M, Lara MF, Segrelles C, Ruiz S, Moral M et al. Spontaneous squamous cell carcinoma induced by the somatic inactivation of retinoblastoma and Trp53 tumor suppressors. *Cancer Res* 2008; **68**: 683–692.
- Lara MF, Santos M, Ruiz S, Segrelles C, Moral M, Martinez-Cruz AB et al. p107 acts as a tumor suppressor in pRb-deficient epidermis. *Mol Carcinog* 2008; **47**: 105–113.
- Santos M, Ruiz S, Lara MF, Segrelles C, Moral M, Martinez-Cruz AB et al. Susceptibility of pRb-deficient epidermis to chemical skin carcinogenesis is dependent on the p107 allele dosage. *Mol Carcinog* 2008; **47**: 815–821.
- Sage J, Miller AL, Perez-Mancera PA, Wysocki JM, Jacks T. Acute mutation of retinoblastoma gene function is sufficient for cell cycle re-entry. *Nature* 2003; **424**: 223–228.
- Johnson DG, Cress WD, Jakoi L, Nevins JR. Oncogenic capacity of the E2F1 gene. *Proc Natl Acad Sci USA* 1994; **91**: 12823–12827.
- Johnson DG, Schwarz JK, Cress WD, Nevins JR. Expression of transcription factor E2F1 induces quiescent cells to enter S phase. *Nature* 1993; **365**: 349–352.
- Field SJ, Tsai FY, Kuo F, Zubiaga AM, Kaelin Jr WG, Livingston DM et al. E2F-1 functions in mice to promote apoptosis and suppress proliferation. *Cell* 1996; **85**: 549–561.
- Yamasaki L, Jacks T, Bronson R, Goillot E, Harlow E, Dyson NJ. Tumor induction and tissue atrophy in mice lacking E2F-1. *Cell* 1996; **85**: 537–548.
- Yamasaki L, Bronson R, Williams BO, Dyson NJ, Harlow E, Jacks T. Loss of E2F-1 reduces tumorigenesis and extends the lifespan of Rb1(+/–) mice. *Nature genetics* 1998; **18**: 360–364.
- Tsai KY, Hu Y, Macleod KF, Crowley D, Yamasaki L, Jacks T. Mutation of E2f-1 suppresses apoptosis and inappropriate S phase entry and extends survival of Rb-deficient mouse embryos. *Molecular cell* 1998; **2**: 293–304.
- Paramio JM, Segrelles C, Casanova ML, Jorcano JL. Opposite functions for E2F1 and E2F4 in human epidermal keratinocyte differentiation. *J Biol Chem* 2000; **275**: 41219–41226.
- D'Souza SJ, Vespa A, Murkherjee S, Maher A, Pajak A, Dagnino L. E2F-1 is essential for normal epidermal wound repair. *J Biol Chem* 2002; **277**(1): 10626–10632.
- Lorz C, Garcia-Escudero R, Segrelles C, Garin MI, Ariza JM, Santos M et al. A functional role of RB-dependent pathway in the control of quiescence in adult epidermal stem cells revealed by genomic profiling. *Stem cell reviews* 2010; **6**: 162–177.
- Lopez RG, Garcia-Silva S, Moore SJ, Bereshchenko O, Martinez-Cruz AB, Ermakova O et al. C/EBPalpha and beta couple interfollicular keratinocyte proliferation arrest to commitment and terminal differentiation. *Nat Cell Biol* 2009; **11**: 1181–1190.
- Pierce AM, Fisher SM, Conti CJ, Johnson DG. Deregulated expression of E2F1 induces hyperplasia and cooperates with ras in skin tumor development. *Oncogene* 1998; **16**: 1267–1276.
- Pierce AM, Gimenez-Conti IB, Schneider-Broussard R, Martinez LA, Conti CJ, Johnson DG. Increased E2F1 activity induces skin tumors in mice heterozygous and nullizygous for p53. *Proc Natl Acad Sci USA* 1998; **95**: 8858–8863.
- Pierce AM, Schneider-Broussard R, Gimenez-Conti IB, Russell JL, Conti CJ, Johnson DG. E2F1 has both oncogenic and tumor-suppressive properties in a transgenic model. *Mol Cell Biol* 1999; **19**: 6408–6414.
- Wikonkal NM, Remenyik E, Knezevic D, Zhang W, Liu M, Zhao H et al. Inactivating E2f1 reverts apoptosis resistance and cancer sensitivity in Trp53-deficient mice. *Nat Cell Biol* 2003; **5**: 655–660.
- Russell JL, Weakes RL, Berton TR, Johnson DG. E2F1 suppresses skin carcinogenesis via the ARF-p53 pathway. *Oncogene* 2006; **25**: 867–876.
- Lara MF, Garcia-Escudero R, Ruiz S, Santos M, Moral M, Martinez-Cruz AB et al. Gene profiling approaches help to define the specific functions of retinoblastoma family in epidermis. *Mol Carcinog* 2008; **47**: 209–221.
- Lachmann A, Xu H, Krishnan J, Berger SI, Mazloom AR, Ma'ayan A. ChEA: transcription factor regulation inferred from integrating genome-wide ChIP-X experiments. *Bioinformatics* 2010; **26**: 2438–2444.
- O'Guin WM, Sun TT, Manabe M. Interaction of trichohyalin with intermediate filaments: three immunologically defined stages of trichohyalin maturation. *J Invest Dermatol* 1992; **98**: 24–32.
- Ruiz S, Santos M, Paramio JM. Is the loss of pRb essential for the mouse skin carcinogenesis? *Cell Cycle* 2006; **5**: 625–629.
- Morris EJ, Ji JY, Yang F, Di Stefano L, Herr A, Moon NS et al. E2F1 represses beta-catenin transcription and is antagonized by both pRb and CDK8. *Nature* 2008; **455**: 552–556.
- Gat U, DasGupta R, Degenstein L, Fuchs E. De Novo hair follicle morphogenesis and hair tumors in mice expressing a truncated beta-catenin in skin. *Cell* 1998; **95**: 605–614.
- Lo Celso C, Prowse DM, Watt FM. Transient activation of beta-catenin signalling in adult mouse epidermis is sufficient to induce new hair follicles but continuous activation is required to maintain hair follicle tumours. *Development* 2004; **131**: 1787–1799.
- Doglioni C, Piccinin S, Demontis S, Cangi MG, Pecciarini L, Chiarelli C et al. Alterations of beta-catenin pathway in non-melanoma skin tumors: loss of alpha-ABC nuclear reactivity correlates with the presence of beta-catenin gene mutation. *Am J pathol* 2003; **163**: 2277–2287.
- Lowry WE, Blanpain C, Nowak JA, Guasch G, Lewis L, Fuchs E. Defining the impact of beta-catenin/Tcf transactivation on epithelial stem cells. *Genes Dev* 2005; **19**: 1596–1611.
- Huelsken J, Vogel R, Erdmann B, Cotsarelis G, Birchmeier W. beta-Catenin controls hair follicle morphogenesis and stem cell differentiation in the skin. *Cell* 2001; **105**: 533–545.
- Li M, He Y, Dubois W, Wu X, Shi J, Huang J. Distinct regulatory mechanisms and functions for p53-activated and p53-repressed DNA damage response genes in embryonic stem cells. *Molecular cell* 2012; **46**: 30–42.
- Rhodes DR, Kalyana-Sundaram S, Mahavisno V, Varambally R, Yu J, Briggs BB et al. OncoPrint 3.0: genes, pathways, and networks in a collection of 18,000 cancer gene expression profiles. *Neoplasia* 2007; **9**: 166–180.
- Rhodes DR, Yu J, Shanker K, Deshpande N, Varambally R, Ghosh D et al. ONCOMINE: a cancer microarray database and integrated data-mining platform. *Neoplasia* 2004; **6**: 1–6.
- Chong JL, Wenzel PL, Saenz-Robles MT, Nair V, Ferrey A, Hagan JP et al. E2f1-3 switch from activators in progenitor cells to repressors in differentiating cells. *Nature* 2009; **462**: 930–934.
- Chong JL, Tsai SY, Sharma N, Opavsky R, Price R, Wu L et al. E2f3a and E2f3b contribute to the control of cell proliferation and mouse development. *Mol Cell Biol* 2009; **29**: 414–424.
- Saavedra HI, Wu L, de Bruin A, Timmers C, Rosol TJ, Weinstein M et al. Specificity of E2F1, E2F2, and E2F3 in mediating phenotypes induced by loss of Rb. *Cell Growth Differ* 2002; **13**: 215–225.
- Rabbani F, Cordon-Cardo C. Mutation of cell cycle regulators and their impact on superficial bladder cancer. *Urol Clin North Am* 2000; **27**: 83–102ix.
- Rabbani F, Richon VM, Orlov I, Lu ML, Drobnjak M, Dudas M et al. Prognostic significance of transcription factor E2F-1 in bladder cancer: genotypic and phenotypic characterization. *J Natl Cancer Inst* 1999; **91**: 874–881.
- Lee JS, Leem SH, Lee SY, Kim SC, Park ES, Kim SB et al. Expression signature of E2F1 and its associated genes predict superficial to invasive progression of bladder tumors. *J Clin Oncol* 2010; **28**: 2660–2667.
- Rounbehler RJ, Rogers PM, Conti CJ, Johnson DG. Inactivation of E2f1 enhances tumorigenesis in a Myc transgenic model. *Cancer Res* 2002; **62**: 3276–3281.
- Paulson QX, McArthur MJ, Johnson DG. E2F3a stimulates proliferation, p53-independent apoptosis and carcinogenesis in a Transgenic Mouse Model. *Cell Cycle* 2006; **5**: 184–190.
- Ziebold U, Reza T, Caron A, Lees JA. E2F3 contributes both to the inappropriate proliferation and to the apoptosis arising in Rb mutant embryos. *Genes Dev* 2001; **15**: 386–391.

- 45 Ruiz S, Segrelles C, Santos M, Lara MF, Paramio JM. Functional link between retinoblastoma family of proteins and the Wnt signaling pathway in mouse epidermis. *Dev Dyn* 2004; **230**: 410–418.
- 46 Takebe N, Harris PJ, Warren RQ, Ivy SP. Targeting cancer stem cells by inhibiting Wnt, Notch, and Hedgehog pathways. *Nat Rev Clin Oncol* 2011; **8**: 97–106.
- 47 Lobo NA, Shimono Y, Qian D, Clarke MF. The biology of cancer stem cells. *Annu Rev Cell Dev Biol* 2007; **23**: 675–699.
- 48 Clevers H. Wnt/beta-catenin signaling in development and disease. *Cell* 2006; **127**: 469–480.
- 49 Chan EF, Gat U, McNiff JM, Fuchs E. A common human skin tumour is caused by activating mutations in beta-catenin. *Nature genetics* 1999; **21**: 410–413.
- 50 Gandarillas A, Watt FM. c-Myc promotes differentiation of human epidermal stem cells. *Genes Dev* 1997; **11**: 2869–2882.
- 51 Haegebarth A, Clevers H. Wnt signaling, Igr5, and stem cells in the intestine and skin. *Am J pathol* 2009; **174**: 715–721.
- 52 Alonso L, Fuchs E. Stem cells in the skin: waste not, Wnt not. *Genes Dev* 2003; **17**: 1189–1200.
- 53 Lorz C, Segrelles C, Paramio JM. On the origin of epidermal cancers. *Curr Mol med* 2009; **9**: 353–364.
- 54 Ahmad I, Sansom OJ, Leung HY. Exploring molecular genetics of bladder cancer: lessons learned from mouse models. *Dis models mech* 2012; **5**: 323–332.
- 55 Ahmad I, Patel R, Liu Y, Singh LB, Taketo MM, Wu XR *et al*. Ras mutation cooperates with beta-catenin activation to drive bladder tumorigenesis. *Cell death disease* 2011; **2**: e124.
- 56 Ahmad I, Morton JP, Singh LB, Radulescu SM, Ridgway RA, Patel S *et al*. beta-Catenin activation synergizes with PTEN loss to cause bladder cancer formation. *Oncogene* 2011; **30**: 178–189.
- 57 Shin K, Lee J, Guo N, Kim J, Lim A, Qu L *et al*. Hedgehog/Wnt feedback supports regenerative proliferation of epithelial stem cells in bladder. *Nature* 2011; **472**: 110–114.
- 58 Brandt WD, Matsui W, Rosenberg JE, He X, Ling S, Schaeffer EM *et al*. Urothelial carcinoma: stem cells on the edge. *Cancer metastasis rev* 2009; **28**: 291–304.
- 59 Segrelles C, Lu J, Hammann B, Santos M, Moral M, Cascallana JL *et al*. Deregulated activity of akt in epithelial basal cells induces spontaneous tumors and heightened sensitivity to skin carcinogenesis. *Cancer Res* 2007; **67**: 10879–10888.
- 60 Paramio JM, Casanova ML, Segrelles C, Mittnacht S, Lane EB, Jorcano JL. Modulation of cell proliferation by cytokeratins K10 and K16. *Mol Cell Biol* 1999; **19**: 3086–3094.
- 61 Segrelles C, Moral M, Lorz C, Santos M, Lu J, Cascallana JL *et al*. Constitutively active akt induces ectodermal defects and impaired bone morphogenetic protein signaling. *Mol Biol Cell* 2008; **19**: 137–149.
- 62 Lorz C, Segrelles C, Garin M, Paramio JM. Isolation of adult mouse stem keratinocytes using magnetic cell sorting (MACS). *Methods in mol Biol* 2010; **585**: 1–11.
- 63 Saeed AI, Sharov V, White J, Li J, Liang W, Bhagabati N *et al*. TM4: a free, open-source system for microarray data management and analysis. *Biotechniques* 2003; **34**: 374–378.
- 64 Chen R, Li L, Butte AJ. AILUN: reannotating gene expression data automatically. *Nature methods* 2007; **4**: 879.
- 65 Dennis Jr G, Sherman BT, Hosack DA, Yang J, Gao W, Lane HC *et al*. DAVID: Database for Annotation, Visualization, and Integrated Discovery. *Genome Biol* 2003; **4**: P3.
- 66 Hosack DA, Dennis Jr G, Sherman BT, Lane HC, Lempicki RA. Identifying biological themes within lists of genes with EASE. *Genome Biol* 2003; **4**: R70.
- 67 Subramanian A, Tamayo P, Mootha VK, Mukherjee S, Ebert BL, Gillette MA *et al*. Gene set enrichment analysis: a knowledge-based approach for interpreting genome-wide expression profiles. *Proc Natl Acad Sci USA* 2005; **102**: 15545–15550.

Supplementary Information accompanies the paper on the Oncogene website <http://www.nature.com/onc>